Prepositioning of driving simulator motion systems

P. Hansson, A. Stenbeck and A. Kusachov

Swedish National Road and Transport Research Institute,
P.O. Box 8072, SE-402 78, Gothenburg, Sweden
Email: hanssonp@student.chalmers.se
Email: andste@student.chalmers.se
Email: artem.kusachov@vti.se

F. Bruzelius*

Swedish National Road and Transport Research Institute,
P.O. Box 8072, SE-402 78, Gothenburg, Sweden
and
Vehicle Dynamics Group,
Chalmers University of Technology,
Sweden
Email: fredrik.bruzelius@vti.se
*Corresponding author

B. Augusto

Swedish National Road and Transport Research Institute,
P.O. Box 8072, SE-402 78, Gothenburg, Sweden
Email: bruno.augusto@vti.se

Abstract: Motion base driving simulators have limited space in which to recreate the motions of the simulated road vehicle. Conventional motion cueing algorithms strive to centre the cabin in the simulator motion envelope to accommodate accelerations in a worst case scenario while respecting the physical boundaries. Using information about the road ahead one can preposition the cabin to an off-centre point, virtually increasing the available space so that larger motions are made possible. The prepositioning algorithm presented here was developed as an addition to a classical motion cueing algorithm and makes use of road data and vehicle speed to adjust the simulator displacement. Simulations show that the amount of acceleration presented by an *x*, *y*-sled system can, with prepositioning, be increased by up to 25% in longitudinal and 53% in lateral direction for an example road. A comparative study including 12 test subjects indicates that the perceived realism is rated higher with prepositioning.

Keywords: driving simulators; motion cueing; prepositioning.

Reference to this paper should be made as follows: Hansson, P., Stenbeck, A., Kusachov, A., Bruzelius, F. and Augusto, B. (2015) 'Prepositioning of driving simulator motion systems', *Int. J. Vehicle Systems Modelling and Testing*, Vol. 10, No. 3, pp.288–304.

Biographical notes: P. Hansson received his MSc in Systems, Control and Mechatronics from Chalmers University of Technology in 2014.

A. Stenbeck received his MSc in Systems, Control and Mechatronics from Chalmers University of Technology in 2014.

A. Kusachov received his MSc in Systems, Control and Mechatronics from Chalmers University of Technology in 2011. Since 2014, he is a Research Engineer at the Swedish National Road and Transport Research Institute and registered as a PhD student at Chalmers University of Technology. His research interests include modelling and control in vehicle dynamics, and driving simulator motion cueing.

F. Bruzelius obtained his PhD in Control Theory from Chalmers University of Technology in 2004. Currently, he is an Adjunct Professor at the Division of Vehicle Dynamics within the Department of Applied Mechanics, Chalmers University of Technology and holds a researcher position at the Swedish National Road and Transport Research Institute at the Vehicle Engineering group. His research interests include vehicle dynamics, tyre and active safety modelling and testing.

B. Augusto received his MSc in Mechanical Engineering from Instituto Superior Técnico (IST), Portugal. Currently, he is a Research Assistant at the Swedish National Road and Transport Research Institute at the Vehicle Engineering Group. His research interests include vehicle dynamics, driving simulators and active safety modelling and testing.

1 Introduction

A large number of driving simulators of many different types exist throughout the world (see e.g., Hamish and Jamson, 2010; Pinto et al., 2008). They are used for many different purposes like driver training, research on driver behaviour, testing of new infrastructure, development of vehicle subsystems, and even for entertainment (Hamish and Jamson, 2010; Pinto et al., 2008; Al Qaisi and Traechtler, 2012). The benefits of using simulators instead of real vehicles in research, are, apart from the obvious safety aspects, the possibility of strict control and repeatability of the driver environment (Hamish and Jamson, 2010; Pinto et al., 2008).

Because of the many different fields of application and the absence of construction standards, no two driving simulators are alike and each is to be considered as a 'prototype in itself' (Pinto et al., 2008). Despite that, one can easily identify two main categories, static (fixed-base) and dynamic (motion-base) driving simulators (Colombet et al., 2008; Henriksson, 2009; Auberlet et al., 2010). The dynamic driving simulators have motion systems allowing the driver to feel the vehicle movements.

The seemingly most popular types of motion system today are based on so called hexapods or Gough-Stewart platforms (see e.g. Fischer et al., 2010; Hamish and Jamson, 2010; Colombet et al., 2008; Chiew et al., 2009; Fichter et al., 2009). The hexapod consists of a base with six linear hydraulic or electromechanical actuators connected to a moving platform capable of 6-DOF. The drivers cabin is typically placed on top of the platform. The hexapod is usually rather small and its motion envelope is limited. To

overcome this limitation some more advanced driving simulators, e.g. SimIV at the Swedish National Road and Transport Research Institute (Jansson et al., 2014), have the cabin and hexapod placed on top of an *x*, *y*-sled capable of large translational movements in one or two axes (Fischer et al., 2010; Hamish and Jamson, 2010). These simulators are said to have 8 (see Fischer et al., 2010) or 6 + 2 (in Pinto et al., 2008), independent DOF achieving redundancy with the surge and sway displacements from both the hexapod and the *x*, *y*-sled.

Every motion system has physical limits in its motion envelope and it is usually not an option to recreate the simulated motions from a vehicle one-to-one. The motion outputs of the simulated vehicle are filtered and then represented in the motion system. The processing logic is commonly called the motion cueing algorithm. Depending on the available motion system, different approaches can be made. High frequency linear accelerations are, if possible, replicated by a corresponding translational movement in the motion system. Sustained, low frequency accelerations are difficult to represent owing to the limits of the actuators and the available motion envelope. Instead such accelerations are represented by tilting the hexapod to make use of the gravitational component, tilt coordination.

Although tilt coordination is widely used in driving simulators it is a common opinion that it should be handled with care or even be avoided as far as possible (see e.g., Fischer et al., 2010; Fischer et al., 2011, 2012; Chapron and Colinot, 2007). A too high tilt rate will be registered as rotation by the driver instead of as linear acceleration. Rate limiting of the tilt coordination will however give rise to time lag in the perceived accelerations (Fischer et al., 2011).

In this paper, the possibilities to preposition an *x*, *y*-sled to an off-centre starting point for upcoming accelerations and thereby virtually enlarge the motion envelope, are investigated. Hence, a larger part of the accelerations can be represented by linear motion in the *x*, *y*-sled rather than by tilt coordination. The effectiveness of the approach is illustrated through simulations as well as a simulator study with 12 test subjects.

Few references can be found in this topic in the literature. Chapron and Colinot (2007) claim to use a prepositioning technique in the SHERPA simulator using an *x*, *y*-sled. The paper does not give a complete picture of the technique but concludes increased room for motion with prepositioning. Weiß (2006) presents a prepositioning algorithm with discrete offsets intended for use in the DLR driving simulator. Weiß was never able to test his algorithm in the real simulator and Chapron's paper was published before the SHERPA simulator was built. Thus neither paper has any results from experiments with test drivers.

The remainder of the paper is organised as follows. First, a section that introduces motion cueing and human perception in this context. The following section presents the pre-positioning approaches. The final two sections are devoted to the results and the discussion.

2 Motion cueing

The body functions that give a human the sense of motion and orientation can be accredited to a number of different receptors throughout the body. These include visual input through the photo receptors in the eyes, movement and posture via proprioceptors throughout the body and accelerations and orientation via the vestibular system

(Encyclopedia Britannica, 2014). When working with dynamic driving simulators it is the vestibular system, which is sensitive to acceleration, rotation and orientation in the gravitational field, that plays the most important role (Hamish and Jamson, 2010).

The vestibular system is used to register translational and rotational acceleration as well as orientation of the body, or more precisely, the head. It is located in the inner ear and consists of two sets of sensory organs, the semi-circular canals and the otoliths (Encyclopedia Britannica, 2014). There are three semicircular canals which, thanks to their perpendicular configuration, respond to angular velocity in roll, pitch and yaw. The two otoliths on the other hand register linear acceleration. Owing to an ambiguity in the vestibular system there is no difference in perception of linear acceleration and gravitational acceleration resulting from tilting of the head (Hamish and Jamson, 2010). This phenomena is utilised in motion cueing in tilt coordination, described below. Both the semicircular canals and the otoliths have what is called a perceptual threshold, a lower limit of the acceleration for the otoliths or rotational velocity for the semi-circular canals, that can be sensed (Benson et al., 1986). In the motion cueing context it is preferable to avoid cues below the threshold, since they cannot be perceived. For the purpose of prepositioning it is crucial to stay below the perception threshold to avoid rendering false cues, i.e. motion cues that are unprovoked and unexpected.

A study was made to find the threshold of linear acceleration detection was made by Benson et al. (1986). The visual and auditory cues were however suppressed in the experiment and the test subjects were asked to signal not only the detection of motion but also the direction. The mean threshold for linear acceleration detection in the x-axis was found to be 0.063 m/s^2 and in y-axis 0.057 m/s^2. A corresponding study performed by Groen and Bles (2004), showed a threshold for rotational velocities at 3 °/s. There is however another study by Nesti et al. (2012) that indicates that when combined with visual cues that contradict the sensed rotation, as in a driving simulator, rotational velocities up to 6.3 °/s remain unnoticed.

Tilting the cabin around the driver's head and using a component of the gravitational vector will give rise to a perceived linear acceleration in the driver's horizontal reference plane (Hamish and Jamson, 2010). This practice, called tilt coordination (TC), in combination with (non-tilting) visual cues is perceived as a continuous translational acceleration (Fischer et al., 2010; Hamish and Jamson, 2010; Pinto et al., 2008; Murgovski, 2007), see Figure 1. This practice must be performed under the perception threshold for rotation in order avoid presenting false cues, motion sickness or other side effects. It is a common opinion that tilt coordination should be handled with care or even be avoided as much as possible, i.e. only using it to represent low frequency linear accelerations (Fischer et al., 2010, 2011, 2012; Chapron and Colinot, 2007).

The high frequency part of the translational acceleration of the simulated vehicle is represented by translational movement in the motion system. The low frequency translational part and high frequency rotational rate (in roll and pitch) are represented by angular movement of the motion system. This is achieved by filtering the acceleration signals from the simulated vehicle, a_{Vh}, through high- and low-pass filters. The desired angular rates, ω_{Vh}, from the vehicle model are also high pass filtered to respect the limitations of the motion envelope. When implemented, the filters are generally modified with scaling and limiters etc. (Reid and Nahon, 1985). The washout filter is responsible for returning the motion system to its neutral position, ideally through movements below the human perceptional threshold.

Figure 1 Tilt coordination principal sketch to simulate acceleration, observe that $a_{TC} < 0$

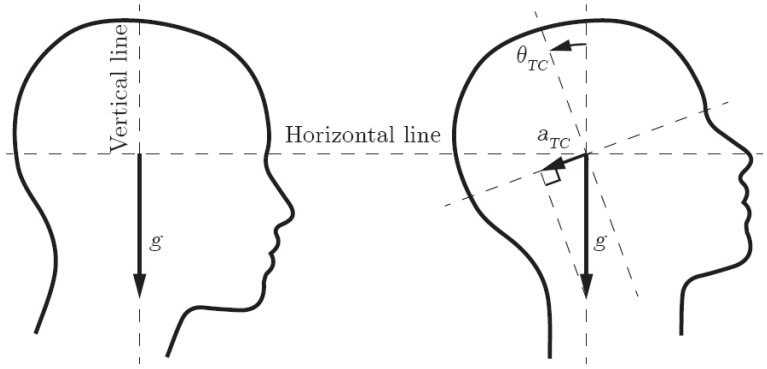

The classical motion cueing algorithm was originally developed for use in 6-DOF motion systems, i.e. only a hexapod. If an additional *x*, *y*-sled is added a variant of the classical algorithm can be used, which is a system of filters that split the vehicle accelerations frequency range between normal translations and tilt coordination. An additional frequency splitting is introduced of the accelerations in the surge and sway directions, the middle frequencies are passed to the *x*, *y*-sled. A simplified version of the motion cueing algorithm, MCA, used in the lateral and longitudinal directions can be seen in Figure 2. This algorithm is further on used in this paper and will be discussed more in detail below.

Figure 2 Principal block diagram of the motion cueing algorithm used here (see online version for colours)

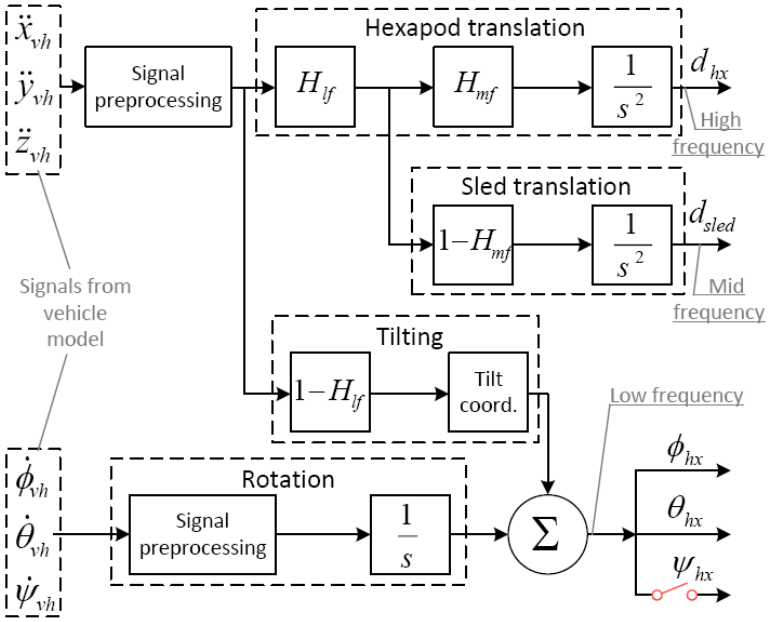

The inputs to the system, the translational accelerations a_{Vh} and rotational velocities ω_{Vh} of the simulated vehicle, are first scaled and limited in order to keep the motion system within its physical boundaries. The angular velocities can only be represented by the hexapod and are simply scaled, limited and integrated to obtain the desired angles β_{Hx}. The translational accelerations are divided into high-, middle- and low frequency components. The low frequency parts are separated by the high pass filter H_{lf} and its complementary filter $1 - H_{lf}$, with cut-off frequency ω_{lf}. The high frequency part then undergo the similar treatment again by the complementary filters H_{mf} and $1 - H_{mf}$, with cut-off frequency ω_{mf}. The high- and middle frequency signals are then integrated twice and passed to the hexapod and x, y-sled respectively as position signals. The low frequency part is passed to the tilt coordination and added to the angles of the hexapod.

The motion cueing system can be tuned by adjusting the scaling, limits and cut-off frequencies of the filters. There is also the washout filter itself, which is excluded in Figure 2, which also has tunable cut off frequencies that influence the performance of the system. Tuning of a motion cueing system can be difficult and arduous since few objective validation methods exist. The system needs to be validated by human perception, i.e. tests with human test subjects have to be made.

3 Prepositioning

One of the main challenges in motion cueing is the difficulty of reproducing large vehicular movement in the limited work space of the simulators motion system. In general it is advised to avoid tilt coordination as far as possible owing to the risk of introducing false cues (Fischer et al., 2010, 2011, 2012; Chapron and Colinot, 2007). By predicting which manoeuvres that are likely to occur, e.g. acceleration, braking, turning etc., one can preposition the motion system accordingly and thus being able to represent a larger, compared to conventional algorithms, part of the simulated vehicles movements. For driving simulators this is of interest primarily for movements in the surge, sway or yaw directions since road vehicles generally experience limited movement in the heave, roll and pitch directions. The motion cueing system then needs to take the extra available space into account to be able to generate a larger movement in these directions.

A hexapod can represent movements in all these directions but with fairly limited stroke. Therefore all the prepositioning is done by the x, y-sled. The most significant movements that need to be represented by the motion system are acceleration, braking and turning. Since acceleration and braking generally generate movements along the vehicle's x-axis and turning along the y-axis, the prepositioning is divided into two algorithms, one lateral and one longitudinal. The lateral prepositioning depends on both the curvature of the road and the current vehicle velocity and will be referred to as road dependent prepositioning while the longitudinal will be referred to as velocity dependent prepositioning. Both these algorithms share the following three tasks,

1 predict future events, i.e. upcoming curves, braking, etc.

2 find the desired position of the platform to best represent the predicted event

3 move to the desired position, before the event occurs, without the driver noticing.

Even though the first two tasks differ substantially between the longitudinal and lateral strategies, task three can be reused for both cases. The two developed and implemented strategies will be presented in the following sections.

3.1 Velocity dependent, longitudinal prepositioning

The *x*, *y*-sled needs to be prepositioned to prepare for driver action. In general this means positioning the *x*, *y*-sled at a point on the *x*-axis from which the driver can either increase speed or brake without hitting the motion system boundaries.

Finding the longitudinal preposition requires knowledge about the vehicle model and its capabilities in terms of acceleration and braking performance. Here we use a model, see Bruzelius et al. (2013), which is parameterised as a Saab 93 with a petrol engine where the engine's maximum torque is described by a simple function of the engine speed. Figure 3(a) shows the maximum acceleration curves for the five different gears as a function of the vehicle velocity converted to km/h and assuming zero tire slip.

The prepositioning in the *x*-axis is designed for the worst case scenario, i.e. the maximum possible accelerations at different vehicle velocities. A function based on the maximum values of the different gear settings is selected. The simple function was fitted to the torque maxima and saturated at 6 m/s^2 as $a_a(v_{Vh}) = \min\{51.84v_{Vh}^{-1}, 6\}$. The obtained curve is plotted in Figure 3(b). The maximum braking acceleration of the vehicle is set to $a_b(v_{Vh}) = -5$ m/s^2 for all vehicle speeds to cover normal driving.

Figure 3 Vehicle acceleration model, (a) $a_{pp,\max}$ curve fitted to max points (b) mean possible longitudinal acceleration curve (see online version for colours)

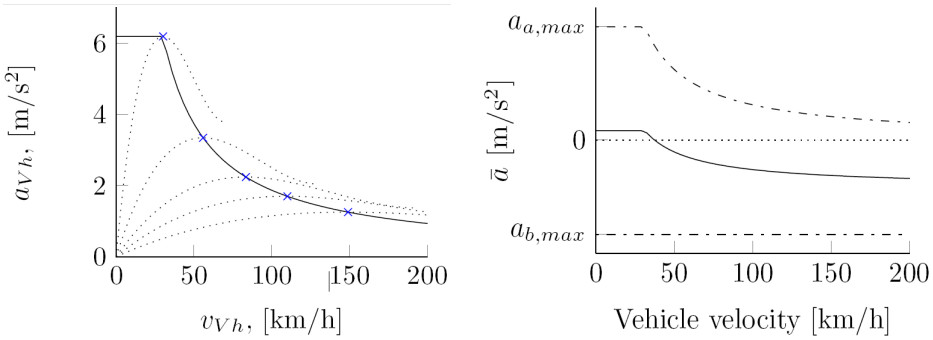

(a) (b)

Since it is not possible to predict if an acceleration or braking will occur at any instant in time, one needs to take both possibilities into account. An action to consider the asymmetry between braking and acceleration capabilities of the vehicle (i.e. a_a and a_b) is to position the *x*, *y*-sled accordingly. This means for example for high speeds that there is no risk of high accelerations and the *x*, *y*-sled can be moved forward relative the to zero (centre) position. More generally, the prepositioning x_{pp} can be formulated as,

$$x_{pp}(v_{Vh}) = \bar{a}(v_{Vh}) \frac{x_{pp,\max}}{\max(\bar{a}_{\max}, |\bar{a}_{\min}|)}. \quad (1)$$

where $\bar{a}(V_{Vh})$ is the mean of the braking and acceleration capabilities,

$$\bar{a}(v_{Vh}) = \frac{a_a(v_{Vh}) + a_b(v_{Vh})}{2}$$

and $\bar{a}_{\max}$ and $\bar{a}_{\min}$ are the maximum and minimum values of the mean w.r.t. speed, see Figure 3(b). This will for every velocity v_{Vh} generate an longitudinal preposition value in the span $[-x_{pp,\min}, x_{pp,\max}]$. The value is then subjected to acceleration limiting to keep the motion below the human perceptual threshold before it is passed on to the motion system.

3.2 Road and velocity dependent, lateral prepositioning

The future lateral accelerations generated by the simulated vehicle are to a large extent determined by the upcoming road curvatures. In driving simulators roads are most often described by a high level definition such as the OpenDrive format (see Dupuis et al., 2013). The shape of the upcoming road is easily accessible from this format and, for example, curvature can be extracted at a distance dependent time t_h ahead of the simulated vehicle.

The lateral acceleration a_n of a point mass with speed v_s in a curve with curvature C is given by,

$$a_n = Cv_s^2. \tag{2}$$

By assuming constant speed for a coming period of t_h it is possible to calculate an upcoming lateral acceleration likely to occur. In order to predict an actual motion to be represented in the motion system, the predicted upcoming acceleration is subjected to the same scaling and limiting as is done in the MCA. Since the prepositioning algorithm is limited to motion in the x, y-sled it uses the same filter used to split the accelerations by frequency in the MCA, letting through only the middle frequency parts of the signal. This ensures that prepositioning is done only for accelerations that will be represented by the x, y-sled. The obtained predicted accelerations are then integrated twice to achieve a position signal and then subjected to a saturation which limits the signal to not exceed $\pm y_{pp,\max}$, i.e. the maximum preposition displacement.

It is desirable to preposition the system according to the maximum acceleration predicted within the given time horizon t_h. The time horizon is chosen as the time required to move the x, y-sled to a preposition in a worst case scenario. This implies that one cannot simply take the signal y_{pp} calculated above as a reference. In every simulation step the current calculated y_{pp} is checked against the highest value within the prediction horizon, y_{ref}. y_{ref} is also checked against the acceleration limited current output of the prepositioning system to see if the reference is reached. The time at which the reference displacement should occur, t_{ref} is within the prediction horizon and has not passed. If any of these three conditions are fulfilled y_{ref} and t_{ref} are updated according to

$$y_{ref} = y_{pp} \text{ and } t_{ref} = t.$$

The above procedure will enable a larger virtual motion envelope and larger portion of the motion presented in the sled. More on that in Section 3.4.

3.3 Acceleration and jerk limitation

The third and final task of the prepositioning algorithm is to make the x, y-sled reach the desired preposition before the intended acceleration is to be represented, without the driver sensing prepositioning motion. Moving the driver's cabin without the driver noticing is a challenge that requires knowledge about the human physiology and motion perception. The horizontal linear acceleration perception threshold of a human lies around 0.05 m/s^2 (Benson et al., 1986). Jerk, the derivative of acceleration, has effects on both the perceived strength of motion and linear acceleration detection thresholds (Fischer et al., 2012; Haycock and Grant, 2007). The detection threshold levels presented by Benson et al. (1986) are therefore to be considered sensitive to combinations of acceleration and jerk although there are no figures on the jerk limits available. The unarguably optimal way to reach the desired preposition with initial and target velocity of zero is to maximise the acceleration and jerk for half the distance and then invert to brake the rest of the distance. This corresponds to a so called bang-bang solution to an optimal control minimum time problem with limited second and third derivatives.

A strategy found in Fischer (2009) and Hippe (2007) is implemented to achieve the bang-bang behaviour of the prepositioning, see Figure 4. Two nonlinearities are introduced to limit the acceleration and the jerk. The oscillations introduced by the nonlinearities are controlled via a PD controller with a feed forward term. The implementation introduces delays between the input and the output but it is not considered a big issue here as the prepositioning is not intended to be perceived by the driver.

Figure 4 Principal block diagram of the acceleration and jerk limiter

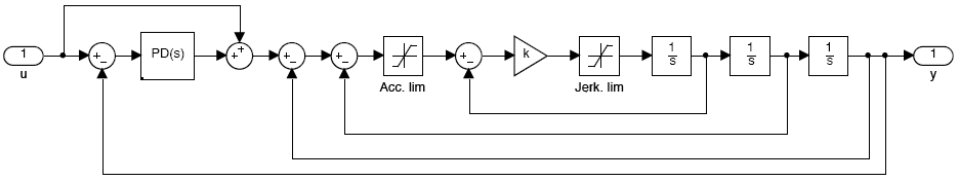

The maximum allowed acceleration in each direction is denoted a_{lim} and the maximum jerk j_{lim}. Since j_{lim} as opposed to a_{lim} cannot be set to a scientifically motivated number, it has to be empirically studied. This is further described in the proceeding section.

Figure 5 Longitudinal prepositioning in real test drive signal (see online version for colours)

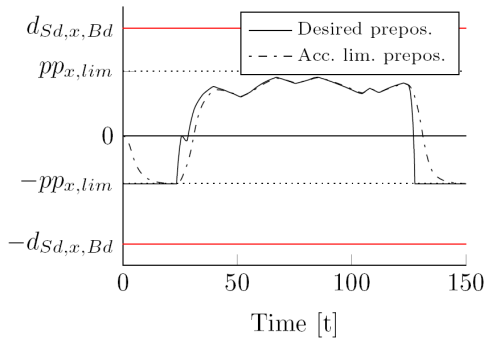

The maximum prepositioning acceleration is set to a_{lim} = 0.05 m/s^2 which is below the human horizontal perception threshold. The PD controller is tuned for an optimal positioning of a maximum prepositioning step of 3 m, which represents a motion from one boundary to the opposite in the prepositioning motion envelope. The motion envelope was chosen to have large margins to the physical boundaries (5 m) as there is a possibility to fail prepositioning within the time frame and maximum acceleration. In Figure 5, one can see the calculated desired longitudinal preposition together with the actual, acceleration limited preposition. The calculation is based on a test drive in the simulator. It shows a delay in the acceleration limited signal but it still manages to follow the reference within acceptable levels for this application. It should be noted that the longitudinal and lateral cases are treated separately and under certain combined conditions the perceptual threshold might be violated. This is not further investigated.

3.4 Expanding the motion envelope

In order to make use of the improved motion envelope of the *x*, *y*-sled system to present accelerations one need to re-tune the MCA. This can be done in basically three ways: altering the scaling factors of the accelerations, changing the limits or changing the cut off frequencies of the motion cueing filters or a combination of the three. The most straight forward option is to alter the cut off frequencies as they will have a controlled impact on the all components of the motion representation rather than emphasising e.g. the *x*, *y*-sled.

It is therefore of primary interest to transfer energy from the low frequency parts, i.e. the accelerations represented by tilt coordination, to the middle frequency part and represent it in the *x*, *y*-sled. With this approach the tilt coordination part of the accelerations will set in later and there are good chances of reducing or in part eliminating the false cues generated by tilt rates above the perception threshold.

In practice, this means altering the parameter ω_{lf} which is the cut off frequency of the high pass filter H_{lf} used in the frequency splitting part of the MCA described earlier. The boundaries of the prepositioning motion envelope are set in accordance to the hardware limitations of the motion system. The offline tuning of w_{lf} was done using a typical test run.

4 Results

Validity of driving simulators can, in general, not be evaluated without the use of test subjects in designed tests. Part of the performance of the preposition can however be objectively assessed, namely the use of tilt coordination and the achieved tilt rate. This section is devoted to measure the performance of the proposed prepositioning algorithms in a simulator study as well as the objective measures through desktop simulations.

4.1 Desktop simulations

Three test runs were made in the simulator to generate signals from the vehicle model. The different test runs, briefly described in the table below, were then used in desktop simulations to measure performance of the proposed prepositioning algorithms.

No.	*Description*	*Used to test*
1	Large accelerations and braking on straight road	x
2	Drive on curvy road	y
3	Drive on curvy road with brakes and accelerations	x and y

Run no. 1 was made to test the longitudinal prepositioning and is therefore characterised by a number of accelerations and braking manoeuvres. Run no. 2 was made to test lateral prepositioning and was therefore driven on a part of a curvy test track. Run no. 3 was made to test the combined lateral and longitudinal prepositioning. The parameters of the prepositioning algorithm are tuned to avoid hitting the boundaries as if the motion system was part of the simulation. The tuning was done using several different test runs and roads and with varying level of accelerations. Tuning of these parameters is always a trade-off, driving too recklessly with any settings will lead to boundaries being hit.

Figure 6(a) shows a comparison between an acceleration represented in the *x*, *y*-sled with and without prepositioning in a six second portion of test run no. 1. Observe that the accelerations of the sled also include compensations for tilt coordinations, etc. Here, one can clearly see the increase in the accelerations rendered in the *x*, *y*-sled as a result of lowered w_{lf}. Figure 6(b) illustrates the decrease and delay in tilt coordination introduced with lowered w_{lf} for longitudinal accelerations during 60 seconds of test run no. 1.

Figure 6 Representation of accelerations in (a) sled and (b) tilt coordination with and without PP

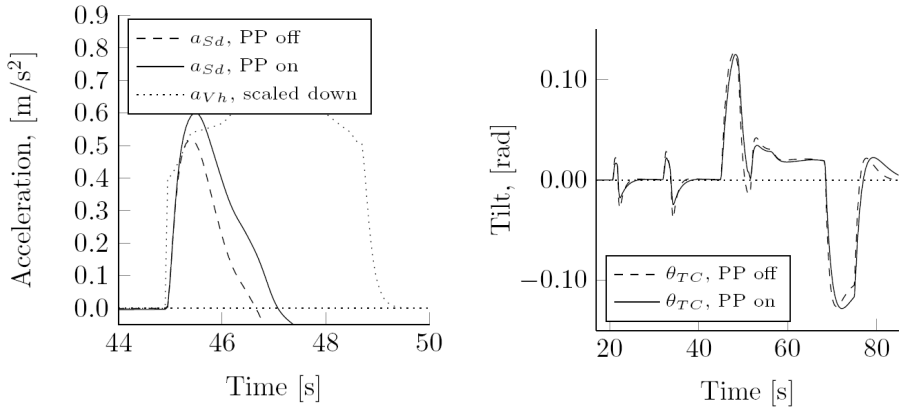

Notes: (a) $a_{Sd,x}$ and $a_{Vh,x}$ with and without prepositioning. 6 s portion of drive no. 1.
(b) θ_{TC} with and without prepositioning. 60 s of drive no. 1.

It is evident that more acceleration is represented in the *x*, *y*-sled and less in tilt coordination. The tilt coordination comes into play later and the tilt rate, i.e. the slope of the curve in Figure 6(b), is lower when the prepositioning algorithm is active. The peak tilt rates at the different test runs are further discussed later in this section.

The possibility to represent more acceleration in the *x*, *y*-sled, i.e. lowering ω_{lf} results in larger amplitudes of motions which without prepositioning would lead to the *x*, *y*-sled reaching its boundaries.

Table 1 Results, drive no. 1

	Unit	*PP off*	*PP on*	*Change*
$a_{Sd,x,RMS}$	m/s^2	0.176	0.220	+25%
$a_{Sd,x,\max}$	m/s^2	0.919	0.998	+9%
$\omega_{TC,\max}$	°/s	7.20	5.05	–29.9%

The increase in total and maximum acceleration rendered in the *x*, *y*-sled and decrease in tilt coordination compared with prepositioning off are presented in Table 1, where $a_{Sd,x,RMS}$ is the root mean square and $a_{Sd,x,\max}$ and $\omega_{TC,\max}$ are the maximum value of the acceleration of the *x*, *y*-sled in the x direction and the tilt rate of the motion system due to tilt coordination respectively. An increase in $a_{Sd,x,RMS}$ by 25 % together with a decrease in the peak tilt rate by almost 30% can be seen.

Testing of the lateral prepositioning, which is based on prediction of lateral accelerations based on future road data, is done in a very curvy, race track like, road. In Figure 7, a part of the run is shown. As one can see there are both higher and longer sustained accelerations when the prepositioning is used. The accelerations from the prepositioning algorithm is subtracted from the *x*, *y*-sled accelerations in the plot to illustrate only the desired accelerations. Note that when prepositioning is on, a lower cut off frequency ω_{lf} is used. Using the same low ω_{lf} would make the case without prepositioning hitting the boundary.

Figure 7 Lateral acceleration comparison with and without prepositioning

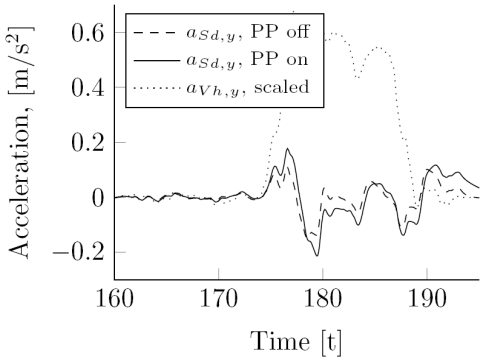

Note: Drive no. 2. Vehicle acceleration scaled by MCA scaling factor.

The increase in total and maximum acceleration rendered in the *x*, *y*-sled and decrease in maximum tilt coordination compared with prepositioning off are presented in Table 2.

Table 2 Results, drive no. 2

	Unit	*PP off*	*PP on*	*Change*
$a_{Sd,y,RMS}$	m/s^2	0.047	0.072	+53%
$a_{Sd,y,\max}$	m/s^2	0.328	0.397	+21%
$\omega_{TC,\max}$	°/s	4.45	3.55	–20.2%

Test run no. 3 was made in order to evaluate concurrent lateral and longitudinal prepositioning. The test road was the same as in test run no. 2 but with the addition of a number of extra brakings and accelerations.

Table 3 Results, drive no. 3

	Unit	*PP off*	*PP on*	*Change*
$a_{Sd,x,RMS}$	m/s^2	0.243	0.267	+10%
$a_{Sd,y,RMS}$	m/s^2	0.047	0.067	+44%
$a_{Sd,x,\max}$	m/s^2	1.003	1.095	+9%
$a_{Sd,y,\max}$	m/s^2	0.342	0.451	+32%
$\omega_{TC,\max}$	°/s	8.05	6.33	–21%

The increase in total and maximum accelerations rendered in the *x*, *y*-sled and the maximum tilt rate, in any direction, compared with prepositioning off are presented in Table 3.

To better visualise the effects of both prepositioning and the change in !lf , plots of the *x*, *y*-sled displacement in both longitudinal and lateral direction during the entire test run are shown in Figures 8(a), 8(b) and 8(c). It is clear from these plots that the space utilisation is improved by the *x*, *y*-sled when the prepositioning is used.

Figure 8 *x*, *y*-plot of sled displacement during drive no. 3, (a) standard ω_{lf} (b) lowered ω_{lf}, near boundary (c) lowered ω_{lf} + PP (see online version for colours)

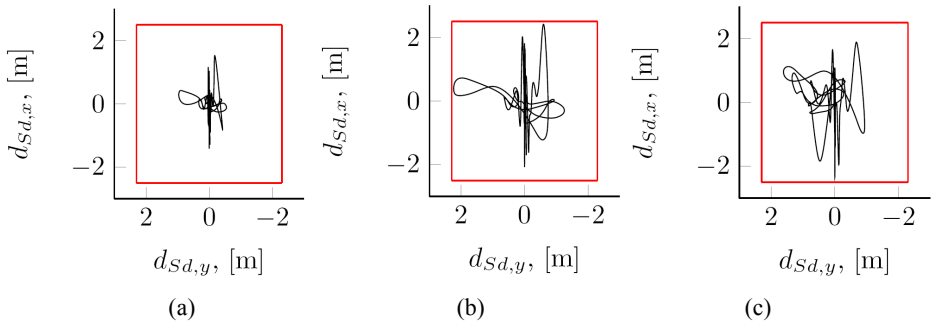

4.2 The driving simulator study

The perceived validity or realism of any simulator depends on human perception. There is no good objective way to measure it but to let unbiased test subjects drive and validate the simulator (Fischer et al., 2012; Henriksson, 2009; Kemeny and Panerai, 2003). The experiment presented here is in form of a psychophysical face validation, designed to fully test if the introduced prepositioning features actually improve the realism.

12 test subjects drove the SimIV simulator two times each, alternating with and without prepositioning in a randomised order. Directly after both test runs they were asked to evaluate it based on their previous, real-life driving experience.

The test scenario was the same for both test runs. The road is of type ‘Swedish rural road’, starts with a straight and finishes with a series of turns. The test subjects were instructed to start driving at 50 km/h and after 1.0 km to increase speed to 70 km/h. After

1.6 km they should stop the car entirely and then resume driving at 50 km/h. After 2.0 km the road becomes 'curvier' and after 4.3 km a completion of the test with a stand still car. Each test run took about five minutes to complete.

Immediately after both runs, the test subjects were given a questionnaire with the following questions,

1 Did the acceleration feel realistic?

2 Did the braking feel realistic?

3 Did the turning feel realistic?

4 Did you experience any unprovoked motions?

5 Did you feel nauseous?

The used scale for rating was from 1 to 7 where 1 corresponds to 'low/bad' and 7 to 'high/good'.

The underlying questions answered indirectly with the questionnaire were:

- Does the increased motion rendering in the x, y-sled increase the validity or realism of the simulator? Questions 1–3.
- Is the prepositioning motion perceivable? Question 4
- Does the increased motion rendering in the x, y-sled reduce motion sickness? Question 5.

The main results from the study are presented in Table 4. It shows the mean result on each question with and without prepositioning and the difference between the two.

Table 4 Questionnaire results, mean scores

Question no.	*1*	*2*	*3*	*4*	*5*
Mean score PP on	5.58	5.33	4.83	2.58	2.83
Mean score PP off	4.50	4.83	4.33	2.92	3.17
Difference	1.08	0.50	0.50	–0.34	–0.34
Significant	Yes	Yes	No	No	No

At first glance there appears to be an improvement in all five categories with the prepositioning turned on. Note that in questions 1–3 a positive difference means an improvement while in questions 4–5 a negative difference means an improvement of the simulator's fidelity.

To ensure if any real difference can be shown a statistical verification is performed with a paired t-test. The paired t-test is used to evaluate if two datasets are significantly different (McDonald, 2009). It is found that at a 95% confidence interval there are statistically significant differences between the case with and without prepositioning in question 1, regarding the realistic feel of acceleration, and in question 2, regarding the realistic feel of the braking. Statistically significant differences could not be established for question 3, regarding turning, question 4, regarding unprovoked motion or for question 5, regarding motion sickness. Since the differences are quite small, further tests are necessary in order to establish statistical significance.

5 Discussion

This paper presents an algorithm that uses *a priori* information for positioning an *x*, *y*-sled of the motion system. By doing so, the motion envelope can be virtually enlarged and a larger part of the acceleration cue can be presented by the simulator. Moving acceleration presentation to the *x*, *y*-sled from the tilt coordination is considered as an improvement since the linear motion of the *x*, *y*-sled does not experience the trade-offs tilt coordination has, e.g. rotational speed versus time to represent the acceleration. The main benefit of the pre-positioning strategy is hence the reduced tilt rate of the tilt coordination.

The algorithm is divided into two parts; one longitudinal and one lateral. The longitudinal part consider the acceleration and braking capabilities of the simulated vehicle and hence it takes the vehicle speed as input. The lateral part is using a constant speed assumption in a look ahead window and determines the prepositioning based on road curvature in this window. The prepositioning parts are actuated through a filter that ensures that the motion is performed under the human perception threshold.

Apart from the existing high number of possible parameters available in the current motion cueing algorithm, there is a new set of parameters introduced with the prepositioning algorithm that can be tuned to improve the functionality. Tuning parameters in this type of simulator is tedious and time consuming. Even though there is potentially much to gain in performance and perceived realism, only minor efforts were put into place.

An alternative approach for longitudinal prepositioning is to analyse the road database in a similar fashion to the lateral prepositioning. The road itself does not contain any specific speed, one can drive as fast or as slow as either the vehicle or the driver can manage. Neither does the road database contain a specific speed. The likelihood of someone driving at the current speed limit or at a speed suiting the current type of road has to be considered. The algorithm can look for road signs indicating speed limits or evaluate the type of road by counting lanes, curvature etc. and prepare the simulator for a possible driving scenario. This has not been investigated further.

The lateral prepositioning algorithm assumes that the driver follows the same lane and only works for the upcoming curvature of that lane. If the road ahead contains multiple lanes that branch out in different direction, slip roads etc. the prepositioning algorithm acts only for the current lane. Although a driver's decisions are hard to predict, a statistical probability could be added to the proposed algorithm in order to preposition the simulator to accommodate all possible future movements.

The velocity input to the lateral prepositioning subsystem is assumed to be constant, i.e. the driver is assumed to keep the same velocity during the entire prediction horizon. This is likely not the case in most situations, as drivers with some self-preservation unarguably lower their vehicle velocity before upcoming sharp curves. This is an area that needs to be investigated further in a future implementation.

The performance of the proposed prepositioning algorithms has been proven here through both simulation and in a simulator study with test subjects. It can be concluded that the algorithm finds an offset preposition both in lateral and longitudinal direction and it moves the *x*, *y*-sled to that point, in time for the subsequent motion and below the human perception threshold. The study also gives evidence of an increased realism in the longitudinal motion, i.e. in acceleration and braking. There are also indications of

increased realism in the lateral movements but enough statistical significance could not be established. Further testing is needed.

References

Al Qaisi, I. and Traechtler, A. (2012) 'Constrained linear quadratic optimal controller for motion control of atmos driving simulator', *Driving Simulation Conference*.

Auberlet, J-M., Pacaux, M-P., Anceaux, F., Plainchault, P. and Rosey, F. (2010) 'The impact of perceptual treatments on lateral control: a study using fixed-base and motion-base driving simulators', *Accident Analysis & Prevention*, Vol. 42, No. 1, pp.166–173.

Benson, A.J., Spencer, M.B. and Stott, J.R. (1986) 'Thresholds for the detection of the direction of whole-body, linear movement in the horizontal plane', *Aviation, Space, and Environmental Medicine*, Vol. 57, No. 11, pp.1088–1096.

Bruzelius, F., Gomez Fernandez, J. and Augusto, B. (2013) 'A basic vehicle dynamics model for driving simulators', *International Journal of Vehicle Systems Modelling and Testing*, Vol. 8, No. 4, pp.364–385.

Chapron, T. and Colinot, J-P. (2007) 'The new PSA Peugeot-Citroen advanced driving simulator overall design and motion cue algorithm', *Proceedings of Driving Simulation Conference*.

Chiew, Y.S., Abdul Jalil, M.K. and Hussein, M. (2009) 'Motion cues visualisation of a motion base for driving simulator', *IEEE International Conference on Robotics and Biomimetics, 2008, ROBIO 2008*, IEEE, pp.1497–1502.

Colombet, F., Dagdelen, M., Reymond, G., Pere, C., Merienne, F. and Kemeny, A. (2008) 'Motion cueing: what is the impact on the driver's behavior', *Proceedings of the Driving Simulation Conference*, pp.171–181.

Dupuis, M. et al. (2013) *OpenDRIVE Format Specification®, Rev. 1.3*, VIRES Simulationstechnologie GmbH, 1.3 ed., August.

Encyclopedia Britannica (2014) [online] http://www.britannica.com/ (accessed 24 June 2014).

Fichter, E.F., Kerr, D.R. and Rees-Jones, J. (2009) 'The Gough-Stewart platform parallel manipulator: a retrospective appreciation', *Proceedings of the Institution of Mechanical Engineers, Part C: Journal of Mechanical Engineering Science*, Vol. 223, No. 1, pp.243–281.

Fischer, M. (2009) *Motion-Cueing-Algorithmen für eine realitätsnahe Bewegungssimulation*, PhD Thesis, Deutsches Zentrum für Luft-und Raumfahrt in der Helmholz-Gemeinschaft, DLR.

Fischer, M., Eriksson, L. and Oeltze, K. (2012) 'Evaluation of methods for measuring speed perception in a driving simulator', *Proceedings of Driving Simulation Conference*, pp.71–93, Institut national de recherche sur les transports et leur sécurité.

Fischer, M., Sehammar, H. and Palmkvist, G. (2011) 'Applied motion cueing strategies for three different types of motion systems', *Journal of Computing and Information Science in Engineering*, Vol. 11, No. 4, 041008.

Fischer, M., Sehammer, H. and Palmkvist, G. (2010) 'Motion cueing for 3-, 6-and 8-degrees-of-freedom motion systems', *Proceedings of the Driving Simulation Conference*, Europe 2010.

Groen, E.L. and Bles, W. (2004) 'How to use body tilt for the simulation of linear self motion', *Journal of Vestibular Research*, Vol. 14, No. 5, pp.375–385.

Hamish, A. and Jamson, J. (2010) *Motion Cueing in Driving Simulators for Research Applications*, PhD Thesis, University of Leeds.

Haycock, B. and Grant, P.R. (2007) 'The influence of jerk on perceived simulator motion strength', *Driving Simulation Conference*.

Henriksson, P. (2009) *Simulatorsjuka-orsak, verkan och åtgärder: en kunskapsöversikt*, Technical Report, VTI, VTI Rapport 587.

Hippe, P. (2007) 'Eine systematische vermeidung der durch stellbegrenzungen ausgelösten probleme', *at-Automatisierungstechnik*, Vol. 55, No. 8, pp.377–393.

Jansson, J., Sandin, J., Augusto, B., Fischer, M., Blissing, B. and Källgren, L. (2014) 'Design and performance of the VTI sim IV', *Driving Simulation Conference*.

Kemeny, A. and Panerai, F. (2003) 'Evaluating perception in driving simulation experiments', *Trends in Cognitive Sciences*, Vol. 7, No. 1, pp.31–37.

McDonald, J.H. (2009) *Handbook of Biological Statistics*, 2nd ed., Sparky House Publishing, Baltimore, Maryland.

Murgovski, N. (2007) *Vehicle Modelling and Washout Filter Tuning for the Chalmers Vehicle Simulator*, Lund University, IEA.

Nesti, A., Masone, C., Barnett-Cowan, M., Giordano, P.R., Bülthoff, H.H. and Pretto, P. (2012) 'Roll rate thresholds and perceived realism in driving simulation', *Proceedings of Driving Simulation Conference*, pp.23–31.

Pinto, M., Cavallo, V. and Ohlmann, T. (2008) 'The development of driving simulators: toward a multisensory solution', *Le travail humain*, Vol. 71, No. 1, pp.62–95.

Reid, L.D. and Nahon, M.A. (1985) *Flight Simulation Motion-base Drive Algorithms: Part 1 – Developing and Testing the Equations*, Institute for Aerospace Studies, Toronto University, UTIAS Report No. 296.

Weiß, C. (2006) *Control of a Dynamic Driving Simulator: Time-Variant Motion Cueing Algorithms and Prepositioning*, Master's Thesis, Deutschen Zentrum für Luft und Raumfahrt.